arXiv:1401.6511v2 [cond-mat.mtrl-sci] 13 Jun 2014

Investigation of thermoelectric properties of half-metallic Co_2MnGe by using first principles calculations

Sonu Sharma and Sudhir K. Pandey

School of Engineering, Indian Institute of Technology Mandi, Kamand - 175005, India
Electronic mail: sonusharma@iitmandi.ac.in

Abstract. By combining the electronic structures obtained from first principles calculations with Boltzmann transport theory we have investigated the electronic, magnetic and transport properties of Co_2MnGe Heusler compound. The density of states plots, dispersion curves and total energy of paramagnetic and ferromagnetic (FM) phases clearly show the half-metallic FM ground state for the compound with an indirect band gap of about 400 meV in the minority spin channel. It has integer value of the magnetic moment equal to 5 μ_B. In the FM phase a very large value ($\sim$550 μV/K) of Seebeck coefficient (S) is obtained for down-spin electrons due to the existence of almost flat conduction band along X to Γ direction. The two current model has been used to find the total S and the obtained value is about 10 μV/K. The calculated values of Seebeck coefficient, resistivity and electronic thermal conductivity show nice agreement with the experimental results.

PACS numbers: 75.50.Cc, 74.25.F-, 74.25.fc, 71.20.-b

1. Introduction

Thermoelectric materials are promising for electronic refrigeration and power generation applications, where heat energy is converted directly into electricity. Also these materials play an important role in a global sustainable energy solution. A good thermoelectric material has high value of the dimensionless figure of merit (ZT), which is given by[1, 2]

$$ZT = S^2\sigma T/(\kappa_e + \kappa_l) \tag{1}$$

where S, σ, T, κ_e and κ_l are the Seebeck coefficient, electrical conductivity, temperature, electronic thermal conductivity and lattice thermal conductivity of the material, respectively. Many materials such as narrow band gap semiconductors, skutterudite, clathrates, complex chalcogenides, silicides and half-metallic ferromagnets have been identified as suitable materials for thermoelectric applications[3]. Recently, half-metallic compounds have attracted much interest because of their exceptional band structures at the Fermi level (E_F). From the electronic band structure point of view, half-metals have metallic character for one spin channel and semiconducting for the other. There exists a high spin-polarization at the E_F and many Heusler alloys belong to this family. The very first time half-metallic ferromagnetism has been introduced by Groot et al.[4] in the NiMnSb half-Heusler alloy. After that many Heusler alloys were found to be half-metallic in different theoretical[5, 6, 7, 8, 9, 10, 11] and experimental[12, 13] studies.

For the spin-polarized materials the total Seebeck coefficient can be evaluated by using two current model[14, 15]. According to this model the expression for total Seebeck coefficient is given by formula:

$$S = [\sigma(\uparrow)S(\uparrow) + \sigma(\downarrow)S(\downarrow)]/[\sigma(\uparrow) + \sigma(\downarrow)] \tag{2}$$

where, S and σ are Seebeck coefficient and electrical conductivity for both the spin channels. Here, it is important to note that the value of S for semiconductors is found to be about 100 times larger than that of the metals[16]. As the half-metallic compounds show metallic behaviour for one spin channel and semiconducting for the other. The total thermopower is expected to be more in these compounds than that of the metals and less than the semiconductors. Experimental studies also suggest that the half-metallic ferromagnetic materials have relatively larger value of the Seebeck coefficient[17, 18]. Co_2MnX-like Heusler alloys are expected to be good thermoelectric materials in the high temperature range because there exits a band gap in the minority spin state of these alloys[19] and they have high Curie temperature[20]. Also it is possible to tune their magnetic properties[6] and E_F position[21] by the substitution of atoms that have similar radii and charges.

For many years, it was very challenging task to calculate accurately the transport properties of materials[22]. Recently, progress has been made by combining the first principles band structure calculations and the Boltzmann transport theory[23, 24, 25]. According to this theory electrical conductivity can be calculated from the electronic structures[25, 26] and usually the electrical conductivity has large dependence on the density of states[27]. Co_2MnGe has a narrow band gap in the minority spin state, so it

is expected that minority spin state will give large value of S than that of the metals. The Curie temperature of the compound is nearly 905 K[17]. In the present work we have studied the electrical transport properties of Co_2MnGe in both the paramagnetic and FM phases for high temperature range.

The full-potential linearized augmented-plane wave methods within local spin density approximation (LSDA) has been employed to calculate the electronic band structures, magnetic states and electronic transport properties of Co_2MnGe. The study of electronic and magnetic properties shows that this compound is half-metallic ferromagnet with the band gap of about 400 meV in the minority spin channel. The temperature dependent electronic transport coefficients are evaluated for both the paramagnetic (PM) and FM phases of the compound. The negative value of S for both phases indicates the presence of N-type charge carriers. In the FM phase the obtained value of S for down spin electrons is $\sim$550 μV/K, which is almost 55 times greater than that of the up spin electrons. The total S is computed by using two current model and its value is found to be about 10 μV/K. The calculated values of S, ρ and κ_e are dominated by majority spin electrons and show fairly good agreement with the available experimental data.

2. Computational details and Crystal structure

The calculations of electronic and magnetic properties have been performed by using the full-potential linearized augmented plane-wave (FP-LAPW) method within the density functional theory (DFT) implemented in WIEN2k code[28]. The exchange-correlation functional has been treated within the local spin density approximation (LSDA) of Perdew and Wang [29]. The muffin-tin radii were set to 2.2 Bohr for Co, Mn and Ge atoms. $R_{MT}K_{MAX}$ which determines the matrix size for convergence was set equal to 7, where R_{MT} is the smallest atomic sphere radii and K_{max} is the plane wave cut-off. The maximum l value (l_{max}) for partial waves used inside atomic spheres was kept 10. The experimental lattice parameter of 5.743 Å[30] has been used in the calculations. The volume of the unit cell was about 284 Bohr^3. The self consistent loop was repeated until the total energy/cell of the system converges to less than 10^{-4} Ry. The $40 \times 40 \times 40$ k-point mesh is used as the accurate calculations of transport properties of metals require the dense sampling of the Brillouin zone. The transport properties of the compound have been calculated by using the BolzTrap code[25] under the constant relaxation time approximation for the charge carriers. The Fermi energy obtained in the self consistent calculations was considered as the chemical potential for the calculation of transport properties of the compound. The values of chemical potential used in the calculation were 0.7926 eV and 0.8051 eV for PM and FM phases, respectively.

Full Heusler compound Co_2MnGe crystallizes in $L2_1$ crystal structure with space group Fm-$3m$. Co atoms are placed on the Wyckoff position 8c (1/4, 1/4, 1/4). Mn and Ge atoms are located at the Wyckoff position 4a (0, 0, 0) and 4b (1/2, 1/2, 1/2), respectively[20]. The cubic $L2_1$ structure consists of four interpenetrating fcc sub-

lattices, two of which are equally occupied by Co atoms. The two Co-site fcc sub-lattices, combine to form a simple cubic sub-lattice. The Mn and Ge atoms occupy alternatively, the centre of the simple cubic sub-lattice resulting in a CsCl-type superstructure[19].

3. Results and discussions

3.1. Paramagnetic Phase

The total density of states (TDOS) and partial density of states (PDOS) plots for the PM phase are shown in Fig. 1. The E_F is represented by dashed line. In Fig. 1(a) the total DOS at E_F is $\sim$7 states/eV/f.u. (f.u. $\equiv$ formula unit) for both the spin channels, which is very large. Such a large value of TDOS at the E_F may be consider as indication of the FM ground state as per the Stoner theory[31]. It is also clear from the figure that the antibonding bands are extended up to about 0.6 eV below E_F. Based on Stoner theory one can easily guess that the total energy of the system will be minimized if there is shifting in spin-up and spin-down bands by about 0.6 eV below and above the E_F, respectively. It give rise to half-metallic FM ground state for the compound. This is also evident from the total energy calculations, where the total energy of FM phase is about 1.1 eV less than the PM phase. From the PDOS of Co atom in Fig. 1(b), it is clear that the contribution of t_{2g} and e_g states at the E_F is $\sim$0.4 states/eV/atom and $\sim$1.3 states/eV/atom, respectively, in both the spin channels. It is also evident from Fig. 1(c) that the Mn t_{2g} and e_g PDOS at E_F is $\sim$1 and 2 states/eV/atom, respectively. The PDOS of Ge atom (Fig. 1(d)) shows that the occupancy at the E_F for p-orbital is $\sim$0.5 states/eV/atom with very small contribution of s and d-orbitals. From these figures it is clear that both t_{2g} and e_g orbitals are mainly contributing to the total DOS at the E_F. These orbitals are expected to be responsible for the FM ground state.

The dispersion curves along the high symmetry directions of the first Brillouin zone are presented in Fig. 2(a). It is evident from the figure that bands labeled by 1, 2 and 3 are lying just above the E_F whereas bands 6, 7 and 8 are lying just below it. Bands 4 and 5 cross the E_F at 8 different k-points. The bands 2-7 are concentrated around W-point in the energy range of about -0.2 to 0.2 eV. Shifting of these bands can minimize the total energy of the system and may lead to the FM ground state for this compound.

In Fig. 2(b-e) temperature induced carrier concentration per unit cell, calculated Seebeck coefficient (S), electrical conductivity (σ/τ) and electronic thermal conductivity (κ_e/τ), where τ is the relaxation time, are displayed for the temperature ranging from 900 K to 1200 K. It is evident from Fig. 2(b) that the temperature induced charge carriers show linear variation with temperature and the absolute value of N decreases from $\sim$ 0.36 e/unit cell at 900 K to $\sim$ 0.007 e/unit cell at 1200 K. Fig. 2(c) shows the linear temperature dependence of the S. The value of S is negative for the entire temperature range, which indicates N-type of charge carriers in the PM phase of the compound. The value of S increases from $\sim$16 μV/K at 900 K to $\sim$26 μV/K at 1200 K. Fig. 2(d and e) represents the temperature variation of the σ/τ

and κ_e/τ. σ/τ shows the slight deviation from the linear temperature dependence, whereas κ_e/τ varies almost linearly with temperature. The value of σ/τ decreases from about 2.43 $\times 10^{20}(\Omega^{-1}m^{-1}s^{-1})$ at 900 K to about 2.41 $\times 10^{20}(\Omega^{-1}m^{-1}s^{-1})$ at 1200 K. The value of κ_e/τ increases from $\sim$0.52 $\times 10^{16}(Wm^{-1}K^{-1}s^{-1})$ at 900 K to $\sim$0.72 $\times 10^{16}(Wm^{-1}K^{-1}s^{-1})$ at 1200 K.

3.2. Ferromagnetic Phase

The TDOS and PDOS for the FM solution are shown in Fig. 3. From the TDOS plots (Fig. 3(a)), it is clear that the majority spin states are occupied at the E_F with occupancy of 1.09 states/eV/f.u. and minority spin states are empty. Thus for spin-up channel this compound is metallic and for spin-down channel it shows semiconducting behaviour. On comparing Fig. 1(a) and 3(a), one can find that in spin-up channel t_{2g} and e_g states shifts towards lower energy whereas, in spin-down channel these states shift towards higher energy as conjectured above. Because of this shifting the almost empty region of spin-down channel about 0.6 eV below the E_F for PM phase, is exactly lying on the E_F in FM phase. Therefore there is creation of band gap in the minority spin channel. This rigid band shift appears to be responsible for the FM ground state in this compound. The Fig. 3 (b-d) show the PDOS plots for the Co, Mn and Ge atoms. In Fig. 3 (b) the PDOS plots for Co 4s, t_{2g} and e_g orbitals are shown. It is clear from the figure that in case of spin-up channel, the Co t_{2g} and e_g states are occupied and for spin-down channel these states are unoccupied. The occupancy at E_F for t_{2g} and e_g states are 0.2 states/eV/atom and 0.07 states/eV/atom, respectively. One can also see the negligible contribution of the other states. The PDOS plot of 4s, t_{2g} and e_g bands of Mn atom is presented in Fig. 3(c). The t_{2g} states mainly contribute ($\sim$0.4 states/eV/atom) at the E_F with negligibly small contribution from other states. This result is quite different from the PM phase where both t_{2g} and e_g orbitals contribute to the E_F. In Fig. 3(d) the density of states for 4s, 4p and 3d-orbitals of Ge atoms are presented which shows negligibly small contribution of these states at the E_F in comparison to t_{2g} state of Co and Mn atoms. This result clearly suggests that t_{2g} electrons of Mn and Co atoms are responsible for the transport behaviour of the compound.

The dispersion curves are presented in Fig. 4 along the high symmetry directions of the first Brillouin zone. These dispersion curves also show the half-metallic ground state of this compound. For spin-up channel in Fig. 4(a), it is clear that bands 1, 2 and 3 cross the E_F at 5 k-points and are responsible for the transport properties of this compound. The bands which are not crossing the E_F will contribute negligibly small to the transport properties. The electrons lying in these bands have energy more than $\sim$1 eV which corresponds to $\sim$12000 K temperature and are not going to influence the transport properties of the compound in the temperature range studied here. Also the shift in chemical potential is about 1 meV which is negligible in comparison to 1 eV mentioned above. Therefore bands crossing the E_F will mainly contribute in the transport properties of the compound. Bands 4 to 8 have shifted deep into the valence

band (VB). For spin-down channel bands 1 to 7 have shifted far away from E_F into the conduction band (CB) and there is a clear cut gap between bands 7 and 8, as indicated in Fig. 4(b). This shifting appears to be mainly responsible for the FM ground state for this compound as stated earlier. The VB maximum is at Γ-point and CB minimum is at X-point, therefore there exists an indirect band gap in the spin-down channel. The computed energy gap with LSDA exchange correlation functional is about 0.40 eV which is smaller than 0.54 eV[9] energy gap obtained by using GGA exchange correlation functional. However, Galanakis et al.[32] have observed no real gap in this full-Heusler alloy, by using the full-potential screened Korringa-Kohn-Rostoker (FSKKR) Greens function method in conjunction with the local spin density approximation. There are three degenerate bands at Γ-point. Along Γ to L and Γ to X direction the degeneracy is partially lifted. The effective mass of the VB is expected to have much smaller value in comparison to the CB as there exits almost flat band in CB along X to Γ direction. The large effective mass for CB is expected to give a very high and negative value of thermopower from the minority spin channel.

The total magnetic moment per formula unit for this compound is 5.0 μ_B with the contribution from Co, Mn, Ge and interstitial region is 1.06, 2.84, -0.02 and 0.05 μ_B, respectively. The total magnetic moment is in agreement with the experimental value [33]. The Mn atom carries the largest magnetic moment and ferromagnetically coupled with the Co atom. Although the magnetic moment of Ge is small but it is coupled antiferromagnetically with Co and Mn atoms. The integer value of total magnetic moment confirms its half metallic character.

The transport coefficients are normally found to be very much sensitive to the k-point sampling of the Brillouin zone. In order to check the k-points dependence of the transport coefficients we have calculated the Seebeck coefficient (S), electrical conductivity (σ/τ) and electronic thermal conductivity (κ_e/τ) at different k-points for spin-up channel. These coefficients correspond to 64000, 125000 and 175616 k-points in the full Brillouin zone are shown in Fig. 5. It is evident from the figure that at low temperature S and σ/τ are very much sensitive to the k-points considered in the calculations whereas κ_e/τ does not show any significant k-point dependence. The values of S and σ/τ above 150 K and 200 K are found to be almost the same for all k-points. Thus the transport coefficients data below 150 K may not be very much reliable. In order to evaluate the low temperature transport behaviour of the compound a careful study is required.

The temperature induced carrier concentration per unit cell, Seebeck coefficient, electrical conductivity and electronic thermal conductivity versus temperature plots corresponding to both the spin channels are presented in Fig. 6. It is clear from Fig. 6(a) that the value of N increases from $\sim$ 0.001 e/unit cell at 150 K to $\sim$ 0.01 e/unit cell at 900 K for spin-up channel. Fig. 6(b) shows that for spin-down channel the value of N increases from about 10^{-6} e/unit cell at 150 K to about 0.03 e/unit cell at 900 K. From Fig. 6(c and d), it is clear that the obtained value of Seebeck coefficient is negative for the entire temperature range and suggesting the presence

of N-type charge carriers. The absolute value of S increases from $\sim 4\mu$V/K at 150 k to $\sim 26\mu$V/K at 900 K for spin-up channel and decreases from $\sim 900\mu$V/K at 150 K to $\sim 274\mu$V/K at 900 K for down spin electrons. At room temperature the obtained values of S are nearly 10 μV/K and 550 μV/K, for spin-up and spin-down channels, respectively. Such a large value of S for spin-down electrons is essentially due to the presence of the almost flat CB along X to Γ direction, as seen in Fig. 4(b). The electrical conductivities for spin-up channel is shown in Fig. 6(e). It is clear from the figure that the conductivity firstly increases from $\sim 4.73\times 10^{20}(\Omega^{-1}m^{-1}s^{-1})$ at 150 K to $\sim 4.75\times 10^{20}(\Omega^{-1}m^{-1}s^{-1})$ at 300 K and then decreases slowly with temperature to the value $\sim 4.70\times 10^{20}(\Omega^{-1}m^{-1}s^{-1})$ at 900 K. At room temperature the value of σ/τ is about $4.75\times 10^{20}(\Omega^{-1}m^{-1}s^{-1})$. The electrical conductivity of spin-down channel is shown in Fig. 6(f). The conductivity increases with increase in temperature from $\sim 2\times 10^{15}(\Omega^{-1}m^{-1}s^{-1})$ at 150 K to $\sim 0.05\times 10^{20}(\Omega^{-1}m^{-1}s^{-1})$ at 900 K and this compound have semiconductor like behaviour for down-spin electrons. At room temperature the value of σ/τ is nearly 0.001 $\times 10^{20}(\Omega^{-1}m^{-1}s^{-1})$ and is very low in comparison to the up spin electrons. The electronic thermal conductivities for both the spin channels are shown in Fig. 6(g and h). For spin-up electrons the thermal conductivity increases linearly from $\sim 0.17\times 10^{16}(Wm^{-1}K^{-1}s^{-1})$ at 150 K to $\sim 1\times 10^{16}(Wm^{-1}K^{-1}s^{-1})$ at 900 K. In case of down-spin electrons the thermal conductivity shows non linear variation and increases from $\sim 2\times 10^{11}(Wm^{-1}K^{-1}s^{-1})$ at 150 K to $\sim 0.04\times 10^{16}(Wm^{-1}K^{-1}s^{-1})$ at 900 K. The room temperature values of κ_e/τ are about 0.34 $\times 10^{16}(Wm^{-1}K^{-1}s^{-1})$ and 0.001 $\times 10^{16}(Wm^{-1}K^{-1}s^{-1})$ for spin-up and spin-down electrons, respectively. For both the spins κ_e/τ increases with increase in temperature.

In order to calculate the total S one can rewrite the equation (2) as,

$$S = S(\uparrow)\{\frac{1+[S(\downarrow)/S(\uparrow)][\sigma(\downarrow)/(\sigma(\uparrow)]}{1+[\sigma(\downarrow)/\sigma(\uparrow)]}\} \tag{3}$$

Using the room temperature values of S and σ in this equation, we find that the ratio of S($\downarrow$) to S($\uparrow$) is about 55, whereas the ratio of $\sigma(\downarrow)$ to $\sigma(\uparrow)$ is about 0.0001. Due to the extremely small value of $\sigma(\downarrow)/(\sigma(\uparrow)]$ in comparison to S($\downarrow$)/S($\uparrow$) the total S is essentially dominated by the value of S($\uparrow$) only. The total S obtained by using equation (3) is presented in Fig. 7. It is evident from the figure that the total S is negative and varies linearly with temperature. The value of S increases from $\sim 4\mu$V/K at 150 K to $\sim 29\mu$V/K at 900 K. The calculated value of S at room temperature is nearly $10\mu VK^{-1}$ and is closer to the experimental values[17, 34]. At low temperature σ/τ and κ_e/τ are mainly contributed by the spin-up channel as evident from Fig. 6(c-f). We have evaluated the ρ and κ_e at room temperature for spin-up channel by using the value of $\tau = 0.5\times 10^{-14}$, because the room temperature value of τ is typically 10^{-14} to 10^{-15} seconds[35]. The calculated values of ρ and κ_e are 0.42 $\mu\Omega m$ and 17.5 $Wm^{-1}K^{-1}$, respectively, which are in good agreement with the experimental values[34].

4. Conclusions

The electronic, magnetic and transport properties of Co_2MnGe have been investigated by combining the electronic structures calculated from first principles methods with the Boltzmann transport theory. The paramagnetic and ferromagnetic density of states plots, electronic band structures and total energy calculations clearly suggest the half-metallic ferromagnetic ground state for the compound. The indirect band gap from Γ to X points is found to be ∼400 meV in the spin-down channel. The total magnetic moment obtained from the calculations is 5 μ_B per formula unit. The integral value of magnetic moment is in accordance with the half-metallic ground state. For spin-down channel the value of S is about 55 times greater than that of the spin-up channel and conductivity is about 0.0001 times smaller. The large value of Seebeck coefficient in the spin-down channel is attributed to the presence of almost flat CB along Γ to X direction. By using two current model the value of total Seebeck coefficient comes out to be ∼10 μV/K and only spin-up channel is found to be responsible for the transport behaviour of the compound. The values of Seebeck coefficient, resistivity and electronic thermal conductivity show fairly good agreement the experimental values.

[1] Y. Pei, X. Shi, A. LaLonde, H. Wang, L. Chen, G. J. Snyder, Nature **473**, 66 (2011).
[2] A. D. LaLonde, Y. Pei, H. Wang and G. J. Snyder, Mater. Today **14**, 526 (2011).
[3] R. Venkatasubramanian, Recent Trends in Thermoelectric Materials Research III, Semiconductors and Semimetals, Vol. 71 (New York: Academic, 2001), p. 175.
[4] R. A. deGroot, F. M. Mueller, P. G. van Engen and K. H. J. Buschow, Phys. Rev. Lett. **50**, 2024 (1983).
[5] I. Galanakis, P. H. Dederichs and N. Papanikolaou, Phys. Rev. B **66**, 134428 (2002).
[6] J. Kübler, A. R. Williams and C. B. Sommers, Phys. Rev. B **28**, 1745 (1983).
[7] S. Ishida, S. Fujii, S. Kashiwagi and S. Asano, J. Phys. Soc. Jpn. **64**, 2152 (1995).
[8] S. Fujii, S. Ishida and S. Asano, J. Phys. Soc. Jpn. **64**, 185 (1995).
[9] S. Picozzi, A. Continenza and A. J. Freeman, Phys. Rev. B **66**, 094421 (2002).
[10] J. Barth, G. H. Fecher, B. Balke, S. Ouardi, T. Graf, C. Felser, A. Shkabko, A. Weidenkaff, P. Klaer, H. J. Elmers, H. Yoshikawa, S. Ueda and K. Kobayashi, Phys. Rev. B **81**, 064404 (2010).
[11] A. Candan, G. Uğur, Z. Charifi, H. Baaziz and M. R. Ellialtıoğlu, J. Alloys Compd. **560**, 215 (2013).
[12] K. E. H. M. Hanssen and P. E. Mijnarends, Phys. Rev. B **34**, 5009 (1986).
[13] M. M. Kirillova, A. A. Makhnev, E. I. Shreder, V. P. Dyakina and N. B. Gorina, Phys. Status Solidi B **187**, 231 (1995).
[14] H. J. Xiang and D. J. Singh, Phys. Rev. B **76**, 195111 (2007).
[15] A. S. Botana, P. M. Botta, C. de la Calle, A. Piñeiro, V. Pardo, D. Baldomir and J. A. Alonso, Phys. Rev. B **83**, 184420 (2011).
[16] C. Wood, Rep. Prog. Phys. **51**, 459 (1988).
[17] B. Balke, S. Ouardi, T. Graf, J. Barth, C. G. F. Blum, G. H. Fecher, A. Shkabko, A. Weidenkaff and C. Felser, Solid State Commun. **150**, 529 (2010).
[18] F. G. Aliev, V. V. Kozyrkov, V. V. Moshchalkov, R. V. Scolozdra and K. Durczewski, Z. Phys. B: Condens. Matter **80**, 353 (1990).
[19] H. C. Kandpal, G. H. Fecher and C. Felser J. Phys. D: Appl. Phys. **40**, 1507 (2007).
[20] P. J. Brown, K. U. Neumann, P. J. Webster and K. R. A. Ziebeck, J. Phys.: Condens. Matter **12**, 1827 (2000).
[21] B. Balke, G. H. Fecher, H. C. Kandpal, C. Felser, K. Kobayashi, E. Ikenaga, J. J. Kim, S. Ueda, Phys. Rev. B **74**, 104405 (2006).

[22] B. R. Nag, Electron Transport in Compound Semiconductors, (Springer-Verlag, Berlin, 1980).
[23] D. J. Singh, Semicond. Semimet. **70**, 125 (2001).
[24] G. K. H. Madsen, J. Am. Chem. Soc. **128**, 12140 (2006).
[25] G. K. H. Madsen and D. J. Singh, Comput. Phys. Commun. **175**, 67 (2006).
[26] U. Mizutani, Electron Theory of Metals Cambridge University Press, Cambridge, 2001.
[27] J. Yang, H. Li, T. Wu, W. Zhang, L. Chen and J. Yang, Adv. Funct. Mater. **18**, 2880 (2008).
[28] P. Blaha, K. Schwarz, G. K. H. Madsen, D. Kvasnicka, and J. Luitz, WIEN2k, An Augmented Plane Wave Plus Local Orbitals Program for Calculating Crystal Properties (Vienna University of Technology, Vienna, 2001).
[29] J. P. Perdew and Y. Wang, Phys. Rev. B **45**, 13244 (1992).
[30] P. J. Webster, J. Phys. Chem. Solids **32**, 1221 (1971).
[31] S. K. Pandey, Phys. Rev. B **81**, 035114 (2010).
[32] I. Galanakis, P. H. Dederichs and N. Papanikolaou, Phys. Rev. B **66**, 174429 (2002).
[33] T. Ambrose, J. J. Krebs and G. A. Prinz, J. Appl. Phys. **87**, 5463 (2000).
[34] S. Ouardi, G. H. Fecher, B. Balke, A. Beleanu, X. Kozina, G. Stryganyuk, C. Felser, W. Klöß, H. Schrader, F. Bernardi, J. Morais, E. Ikenaga, Y. Yamashita, S. Ueda and K. Kobayashi, Phys. Rev. B **84**, 155122 (2011).
[35] N. W. Ashcroft and N. D. Mermin, Solid State Physics, (New York: Saunders College Publishing, 1976) p. 9.

5. Figures

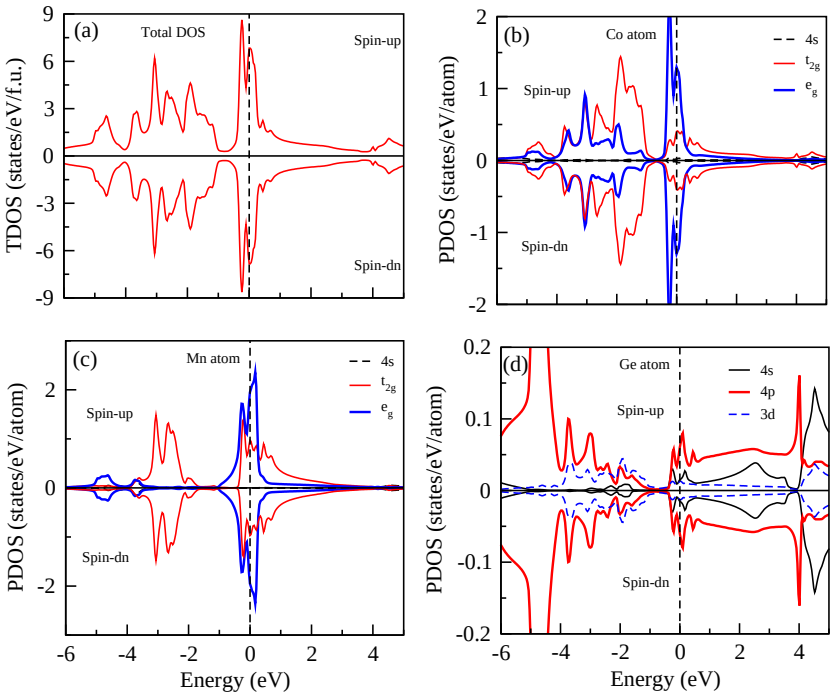

Figure 1. (Color online) Total and partial density of states plots for Co_2MnGe in the paramagnetic phase. Shown are (a) the TDOS plot, (b) PDOS of Co atom, (c) PDOS of Mn atom and (d) PDOS of Ge atom.

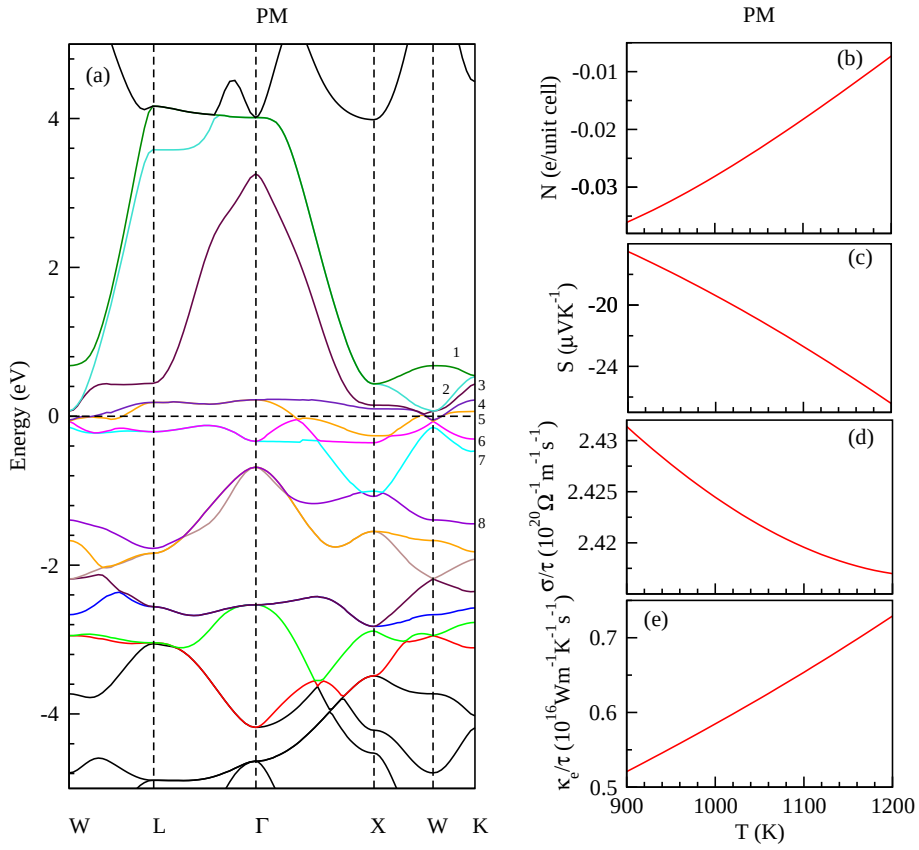

Figure 2. (Color online) Electronic band structure and transport properties of paramagnetic Co_2MnGe. Shown are the (a) electronic band structure, (b) temperature induced carrier concentration per unit cell. Temperature variation of Seebeck coefficient, Electrical conductivity and Electronic thermal conductivity are shown in (c), (d) and (e), respectively.

(b)

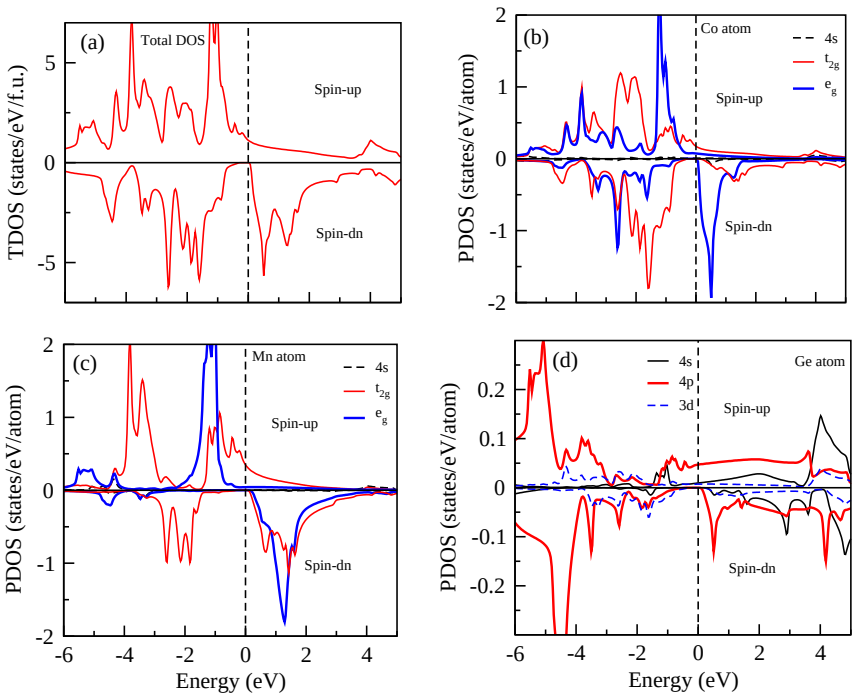

Figure 3. (Color online) Total and partial density of states plots for Co_2MnGe in the ferromagnetic phase. Shown are (a) the TDOS plot, (b) PDOS of Co atom, (c) PDOS of Mn atom and (d) PDOS of Ge atom.

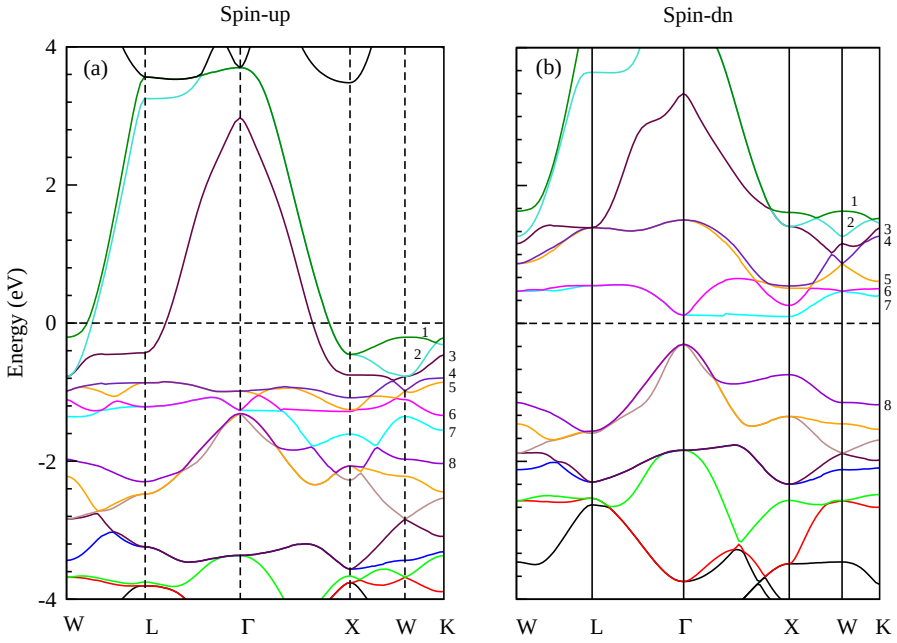

Figure 4. (Color online) Electronic band structures of ferromagnetic Co_2MnGe (a) spin-up channel and (b) spin-down channel.

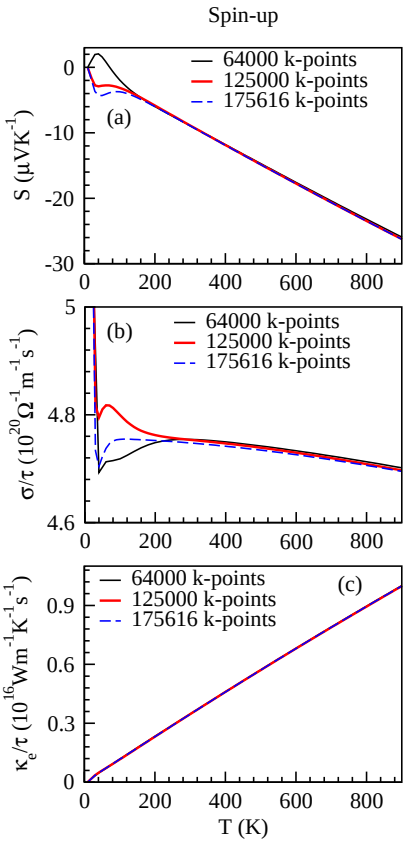

Figure 5. (Color online) k-point dependence of (a) Seebeck coefficient, (b) Electrical conductivity and (c) Electronic thermal conductivity.

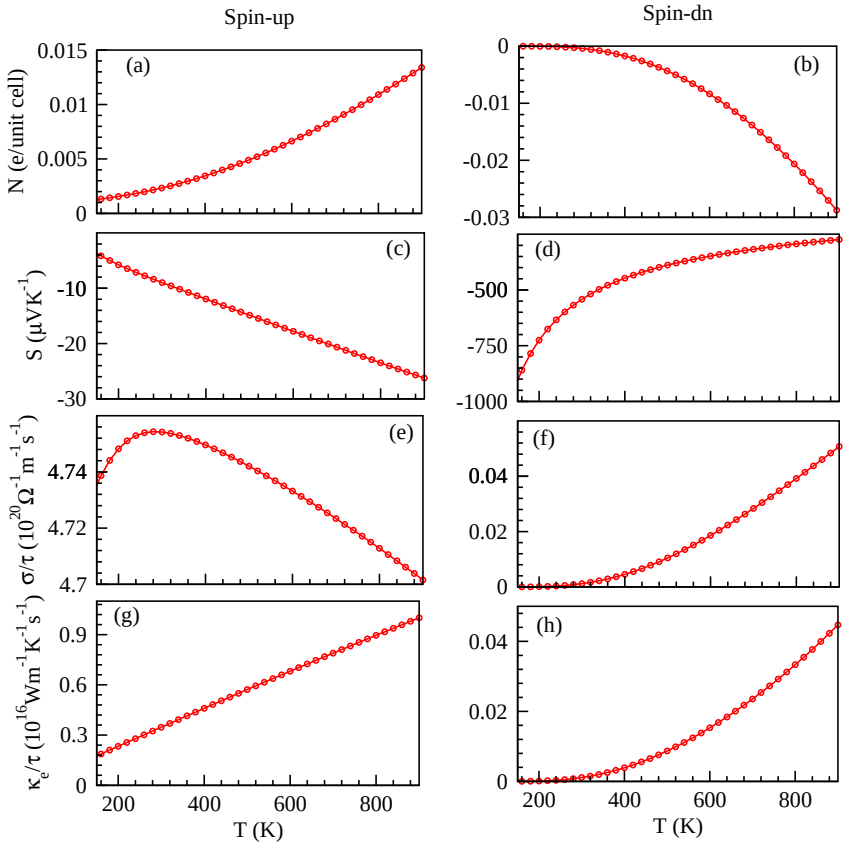

Figure 6. (Color online) Variation of the transport properties in ferromagnetic phase with temperature for spin-up and spin-down channels. Shown are (a and b) temperature induced carrier concentration per unit cell, (c and d) Seebeck coefficient, (e and f) Electrical conductivity and (g and h) Electronic thermal conductivity.

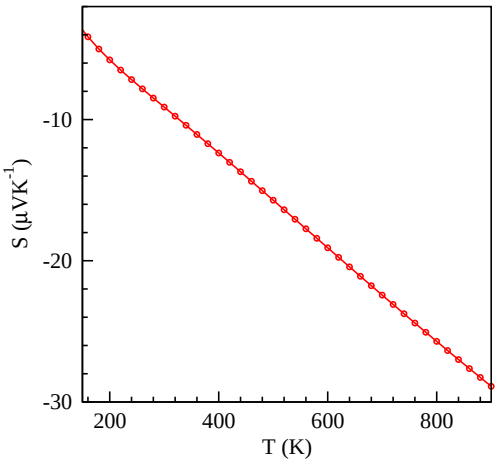

Figure 7. (Color online) Variation of total Seebeck coefficient (S) with temperature.